Article

Not peer-reviewed version

The Effect of 3D-Printed Polylactic Acid Coating Layers on High-Cycle Fatigue Behaviors of AM60 Magnesium Alloys for Additive-Manufactured and Degraded Specimens in Simulated Body Fluid

Seyed Ali Ashraf Talesh and Mohammad Azadi *

Posted Date: 25 December 2023

doi: 10.20944/preprints202312.1814.v1

Keywords: High-cycle fatigue; AM60 magnesium alloy; Polymer coating; Fused deposition modeling; Additive manufacturing; Corrosion; Simulated body fluid

Article

The Effect of 3D-Printed Polylactic Acid Coating Layers on High-Cycle Fatigue Behaviors of AM60 Magnesium Alloys for Additive-Manufactured and Degraded Specimens in Simulated Body Fluid

Seyyed Ali Ashraf Talesh and Mohammad Azadi *

Faculty of Mechanical Engineering, Semnan University, Semnan, Iran
* Correspondence: m_azadi@semnan.ac.ir

Abstract: In the previous work, the pure fatigue behavior of AM60 magnesium alloy (PF-AM60) was compared with the corrosion fatigue behavior of these specimens (CF-AM60). In this research, in continuation of the previous job, the pure fatigue behaviors of AM60 with polylactic acid (PLA) coating (PF-AM60-PLA) and also, corrosion fatigue behaviors of magnesium alloy with PLA coating (CF-AM60-PLA) were evaluated. Polymer coating was made by fused deposition modeling (FDM) with a 3D printer and attached to standard fatigue test specimens with a glue. Then, they were immersed in the simulated body fluid (SBF) for 27 days. In the end, a high-cycle bending fatigue test was performed on samples. The fracture surface of the samples was also observed using the field emission scanning electron microscopy (FESEM). Due to corrosion, the weight of the specimens redcued by an average of 35%. The corrosion rate decreased in the first 7 days and then increased. PF samples with coating had an average of 49% increase in fatigue lifetime. Regarding the CF samples, despite the use of a 10 times stronger solution, the fatigue lifetime of these samples decreased by only 35%. FESEM results also showed cleavage plates and striations. In addition, the separation of the glue from the coating and Mg was observed. Corrosion products including microcracks and holes were seen on the fracture surface of CF specimens, which caused stress concentration and crack growth. Holes caused by the release of gases were also observed in polymer coatings.

Keywords: high-cycle fatigue; AM60 magnesium alloy; polymer coating; fused deposition modeling; additive manufacturing; corrosion; simulated body fluid

1. Introduction

AM60 magnesium alloys have perfect mechanical properties such as strength and high fracture toughness [1,2]. This material has a low density and is biocompatible. For this reason, AM60 were used in structures under corrosion and fatigue loads. Magnesium is used in many industries such as automotive, aerospace, healthcare and biomedical. Magnesium is also used in implants and stents [3–6].

Song et al. [7] searched for a comparison of the corrosion performance of AM60 magnesium alloys in an atmospheric environment, both with and without the application of self-healing coatings. The results indicated that rainwater in scratched areas can acceler-ate corrosion in magnesium. Additionally, it was found that self-healing coatings possess better inhibitive properties. Liu et al. [8] explored the corrosion characteristics of the AM60 magnesium alloy that incorporate either cerium (Ce) or lanthanum (La) when sub-jected to thin electrolyte layers. The smart map analysis confirmed the skeletal structure formation from the rare earth (RE) alloying. Finally, the corrosion pattern observed in AMRE1 alloy indicates the corrosion area, and the application of thin electrolyte layer (TEL) effectively suppresses the development of pitting corrosion. Matsubara et al. [9] found the impact of iron impurity on the corrosion behaviors of AM60 and AM50 magne-sium alloys. The findings suggested that an increase in the Fe/Mn ratio correlated with higher rates of corrosion. That article concluded that these inclusions had a role of initia-tion corrosion points. Xie et al. [10] researched enhancing the anti-corrosion and anti-wear characteristics of AM60 magnesium alloys.

 doi:10.20944/preprints202312.1814.v1

They improved this through ion im-plantation and a gradient duplex coating. The research revealed a significant improving behavior under the corrosion condition in magnesium alloys when it was coated. This improvement was evident in the current density of corrosion. Kumar [11] researched the effects of incorporating hydroxyapatite (HA) into AZ91D, AJ62, and AM60 alloys. The study found that HA, through the formation of complex metal hydroxides, enhances corrosion resistance. As a result, AJ62/3HA and AZ91D/3HA alloys were found as promising bio-material candidates due to their finer grains, exceptional resistance to corrosion, and strong biocompatibility, making them suitable for various applications. Other studies were conducted on the corrosion behavior of the AM60 alloy in the NaCl environment. Researchers in these studies attempted to increase the strength under the corrosion in the AM60 alloys by adding materials such as rare earth cerium and lanthanum metals, organic inhibitors, and mineral inhibitors [12–15].

Akbaripanah et al. [16] studied the impact of the equal channel angular pressing (ECAP) technique besides extrusion on the fatigue characteristics of the AM60 magnesium alloys. In the second pass of ECAP, researchers found that fatigue lifetime increased. This result was important because the improvement was seen in both low cycling and high cycling. Khan et al. [17] investigated the fatigue behavior of anodized AM60 magnesium alloys when exposed to a humid environment. The researchers found that anodized samples under high humidity conditions (80% RH) slightly improved fatigue strength. Hiromoto et al. [18] performed a work on the fatigue properties of bio-absorbable magnesium alloys with hydroxyapatite coatings, formed through the chemical solution deposition method. In the final phase of the research, the investigators discovered that the hydroxyapatite (HAp) coatings on the sample remained intact without developing cracks even after 107 fatigue cycles considering the fatigue limit. This suggested that the HAp coating offered approximately 3% cyclic elongation, showcasing its potential to increase the durability of AZ31 magnesium alloy components in specific applications. Considering the wide range of applications for magnesium alloys, numerous studies were carried out on these materials. As a result, a substantial body of research was dedicated to exploring the corrosion fa-tigue behaviors in the magnesium alloy. Through these investigations, researchers sought to enhance the alloy resistance to corrosion fatigue by altering their composition and micro-structure [19–26].

Shi et al. [27] investigated a novel MAO-PLA coating applied to zinc alloys with the potential for use as an orthopedic implant material. In the research, the Zn-0.5Mn-0.5Mg alloys were subjected to surface modification by micro-arc oxidation (MAO) besides sol-gel PLA techniques. This treatment enhanced osteogenesis and reduced the material toxicity for potential medical applications. Ultimately, based on the results obtained, researchers concluded that the surface modification of the MAO-PLA on the Zn-0.5Mn-0.5Mg alloys appeared to be suitable for improving biocompatibility. Anand et al. [28] assessed biode-gradable composites, Zn-Mg-Mn-(HA), coated with a polymer-ceramics composite (PLA/HA/TiO2) for orthopedic applications. They observed higher corrosion rates in the as-cast sample, 1Mg-1Mn-1HA, than 1Mg-1Mn. However, after applying the polymer-ceramic nanofiber composite coating, the corrosion rates significantly decreased in electrochemical tests. Wang et al. [29] investigated the corrosion resistance of biode-gradable iron and zinc materials by applying a poly(lactic) acid (PLA) coating to use these materials for temporary medical implant applications. The study found that PLA enhances iron (Fe) corrosion rate more effectively than zinc (Zn). This observation is likely attributed to the non-passivating nature of iron in an acidic environment. Beyzavi et al. [30] explored bio-polymer coatings, generating these coatings on the AM60 magnesium alloy with 3D printing by fused deposition modeling (FDM) in their study. These coatings were applied to explore the electrochemical behavior of the treated magnesium alloys. Their data on testing of electrochemical impedance spectroscopy revealed that the transparent Polycaprolactone (PCL) and PLA coatings exhibited the highest impedance. However, all the biodegradable coatings exhibited a significant increase in impedance, approximately 63.1-99.7%, compared to the magnesium alloy.

Based on the conducted studies, it was determined that many researchers had worked in the field of AM60 corrosion, and their goal was to improve corrosion using various methods [7–15], Moreover, studies have shown that the use of biodegradable polymer coatings such as PLA can have

Preprints (www.preprints.org) | NOT PEER-REVIEWED | Posted: 25 December 2023 doi:10.20944/preprints202312.1814.v1

a positive impact on corrosion [27–30], Furthermore, it was disclosed that several studies were carried out in the field of fatigue of AM60 [16–26].

The innovation of this research is to compare the fatigue lifetime of coated Mg after corrosion in SBF with pure Mg.

2. Materials and Methods

2.1. Materials and Manufacturing Method

The primary material used in the present research is a magnesium alloy. Then, the chemical composition of this alloy was determined using a quantometric test, where its results are shown in Table 1. From the comparison of the obtained results with the ASTM B94 standard, it was concluded that the alloy used is AM60. Its field-emission scanning electron microscopy (FESEM) images and energy-dispersive X-ray spectroscopy (EDX) were used for the microscopic evaluations. The related data illustrated that the magnesium matrix is based on Al12Mg17, Al6Mn, and MgO [31,32]. More details are provided in the study [33]. Standard fatigue test samples were made from this alloy by casting method.

Table 1. The quantometry result for AM60 (wt.%).

Mg	Mn	Zn	Si	Al	Ni	Cu
Bulk	0.3	0.07	0.04	5.5	0.004	0.01

After the production of standard fatigue test samples, polymer coatings were made separately and using the fused deposition modeling (FDM) technique. The coating used in this research is polylactic acid (PLA). This polymer is biocompatible. Its melting temperature is 180-230°C and its density is 1240 kg/m^3 [34,35]. The 3D printing parameters of these coatings are presented in Table 2. These parameters were chosen according to the literature [36,37].

Table 2. The 3D printing parameters.

Parameters	Speed (mm/s)	Nozzle temperature (°C)	Bed temperature (°C)	Infill in first and last layer (%)	Infill in inner layer (%)	Layer High (µm)	Nozzle diameter (mm)
Value	50	245	60	100	50	50	0.4

The polymer coatings were attached to magnesium fatigue standard samples using glue. In this research epoxy glue with Megapox 300 Ghafari brand was used. It was shown in research [38] that epoxy adhesives are not harmful to humans. These adhesives are two components and are mixed together in equal proportions. For bonding, the fatigue standard sample was first degreased with dishwashing liquid. Then the adhesive was used between the surface of the base metal and the coating layers. Based on the instructions by the glue manufacturer, the samples were kept in room air for 24 hours. Then the tests were performed. Figure 1 depicts the standard sample of fatigue testing, with and without coating.

Figure 1. The fatigue standard sample with and without coating before corrosion

Preprints (www.preprints.org) | NOT PEER-REVIEWED | Posted: 25 December 2023 doi:10.20944/preprints202312.1814.v1

According to ASTM D4541, adhesion testing was done by the pull-off experiment. An adhesion device made by Defelsko company was used to perform this test. An adhesion test was performed from each sample at three different points. The average of the obtained results, which shows the amount of adhesion between the base metal and the coating, was measured 4.29±0.71. In another research [39], the amount of adhesion between PLA and Mg, which were connected to each other by electrolytic plasma oxidation method, was measured.

2-2. Corrosion Test

Standard fatigue test samples with coating were subjected to corrosion. For this purpose, the specimens were completely immersed in the 1X simulated body fluid (SBF). But with time, no corrosion occurred. Figure 2 shows a corrosion fatigue standard sample with 1X SBF after 30 days. Therefore, 10X SBF was used. The composition table of the SBF solution is depicted in Table 3. Based on this table, the main ions of the SBF solution are Na^+ and Cl. However, due to the presence of other ions, the corrosion effects with NaCl solution will be completely different. For example, the hydrogen element can lead to the production of $Mg(OH)_2$, which does not occur in NaCl solution. The differences between these two solutions have been fully investigated in research [40].

The samples were weighed every day for the first 7 days. Then, on days 13, 20, and 27, the weight of the specimens was recorded. It must be noted that before each weighing, the samples were completely cleaned with a napkin and left in the open air for a few hours to dry completely. Figure 3 shows the fatigue standard sample with coatings after the immersion in SBF environment on different days. In addition, Figure 4 illustrates the specimen after corrosion testing, with and without corrosion products.

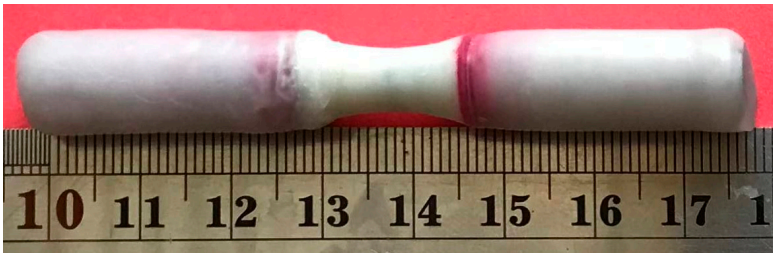

Figure 2. The corrosion fatigue standard sample with 1X SBF after 30 days.

Table 3. The constituent elements of SBF used [41].

Ions	Concentration (mM)	Ions	Concentration (mM)
Mg^{2+}	15.0	HPO_4^{2-}	10.0
K^+	50.0	HCO^{3-}	42.0
Na^+	1420.0	Cl^-	1478.0
Ca^{2+}	25.0	SO_4^{2-}	5.0

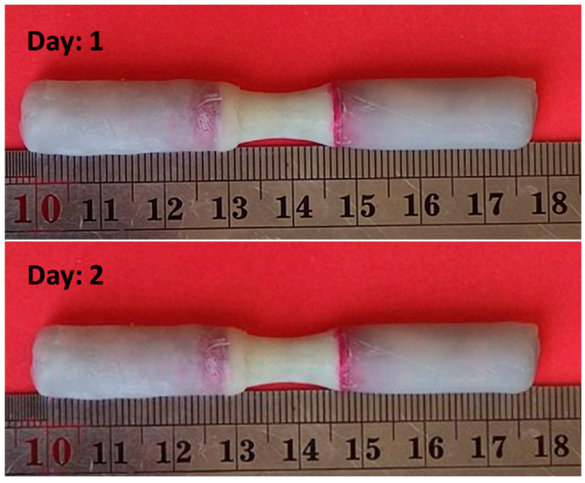

Preprints (www.preprints.org) | NOT PEER-REVIEWED | Posted: 25 December 2023 doi:10.20944/preprints202312.1814.v1

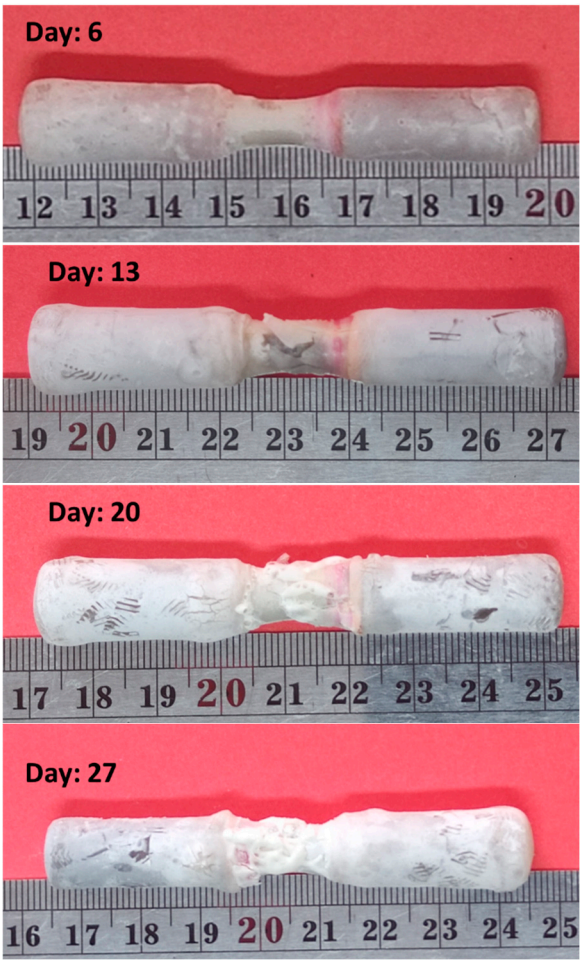

Figure 3. Image of standard samples during corrosion test.

Figure 4. Samples after the corrosion test without corrosion products.

Based on the ASTM-G31-72 standard [42], the rate of corrosion can be calculated in mils per year (MPY) according to Equation 1, as follows,

Preprints (www.preprints.org) | NOT PEER-REVIEWED | Posted: 25 December 2023 doi:10.20944/preprints202312.1814.v1

$$Corrosion\ rate = \frac{KW}{AtD} \quad (1)$$

In this equation, A is the sample area (cm^2), which is exposed to the environment, W is the weight loss (gr), D is the density of the material (gr/cm^3), t is the exposure time (hr), and $K = 3.45\times10^6$ [43].

2.3. Fatigue Test

The high-cycle rotary bending fatigue test ($R=-1$) was performed based on the ISO-1143 and DIN-EN-50113 standards [44,45]. To perform this test, SFT-600 device made by Santam Company was used. All experiments were conducted at room temperature and under a loading frequency of 100 Hz. The map of standard specimens is decpited in Figure 5.

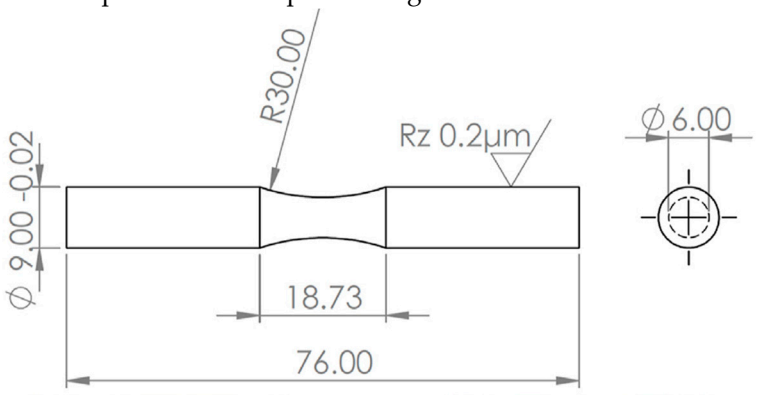

Figure 5. The map of the Fatigue standard specimen.

Fatigue tests were performed for samples under 4 stress levels of 80, 100, 120, and 140 MPa and with a repeatability of 3 tests for each sample. The fatigue limit of magnesium was considered at 60 MPa besides 1 million cycles [44].

2.4. Fracture Surface Analyze

The fracture surfaces of the samples were seen by the field-emission scanning electron microscopy (FESEM), the Sigma 300 model, made in Zeiss, Germany. Before imaging, a gold coating layer was also applied on the specimen surfaces.

3. Results

The samples with the coating were placed in the SBF solution for 27 days. Then, the weight of the specimens was recorded during this period. Figure 6 depicts the change in weight according to the days that the samples were in the solution. According to this figure, the weight of the samples did not change in the first days. However, on some days it decreased, then on the last days the weight of the sample increased. This is due to water absorption by the polymer coating [46]. Hasanpour et al. [47] investigated water absorption and corrosion of pure magnesium and magnesium with PLA. The specimens were immersed in the SBF solution for 30 days. It was concluded that the corrosion rate in samples with PLA is increased due to more water absorption. Balogova et al. [48] for PLA samples showed that the mass of samples increases with increasing water absorption. Redondo et al. [49] also reported water absorption in corrosion tests for PLA samples. Alksne et al. [50] reported swelling and water absorption over time for Composite samples made of PLA+hydroxyapatite (HA) and PLA+bioglass (BG).

Preprints (www.preprints.org) | NOT PEER-REVIEWED | Posted: 25 December 2023 doi:10.20944/preprints202312.1814.v1

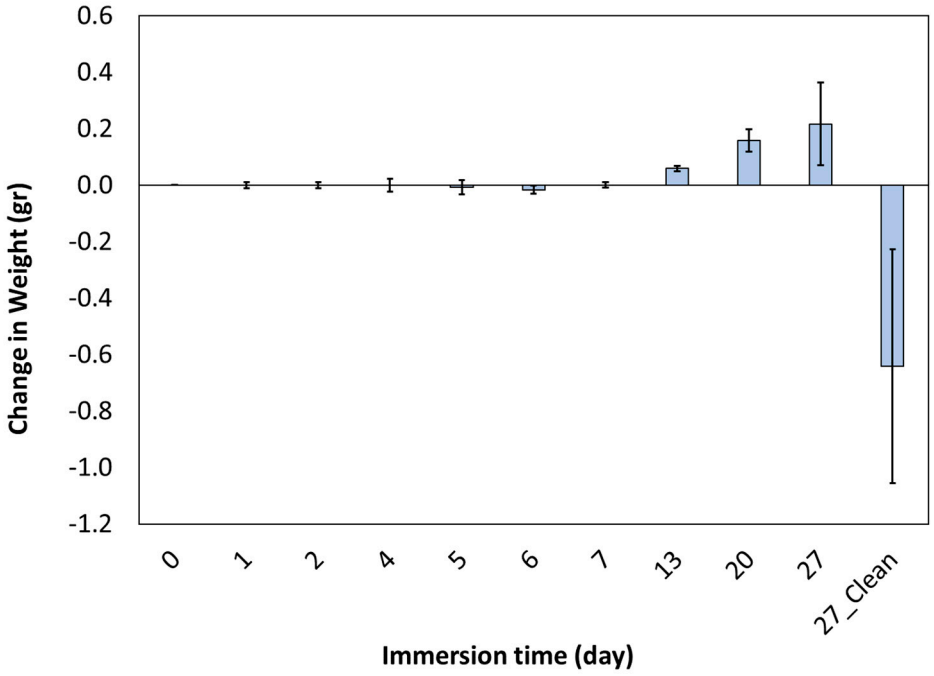

Figure 6. The changes in weight of the corroded specimens.

Figure 7 shows the corrosion rate and the average rate of corrosion. Based on this figure, the corrosion rates decreased over the time. Chor et al. [51] also reported a decrease in the corrosion rate for a sample made of PLA materials over the time. Voicu et al. [52] combined MgZ31 with PLA nanofibers and the corrosion of samples in SBF solution was investigated. The results illustrated that the rate of corrosion decreased with the help of PLA coating. Shi et al. [53] fabricated a PLA layer on the sample by placing AZ31 in the PLA-chloroform solution. The corrosion results demonstrated that the coating layers decreased the corrosion rate.

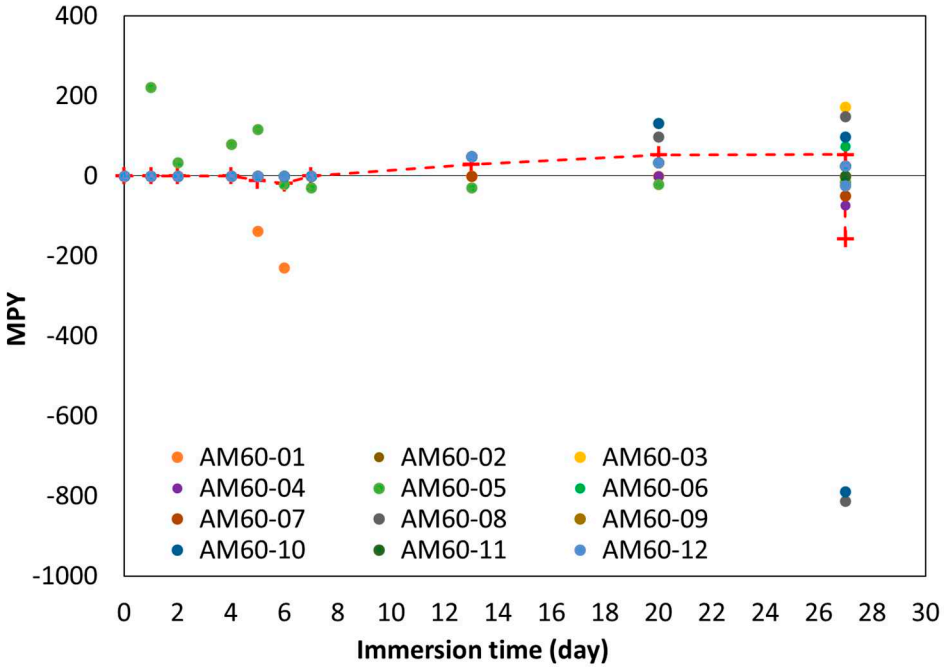

(a)

Preprints (www.preprints.org) | NOT PEER-REVIEWED | Posted: 25 December 2023 doi:10.20944/preprints202312.1814.v1

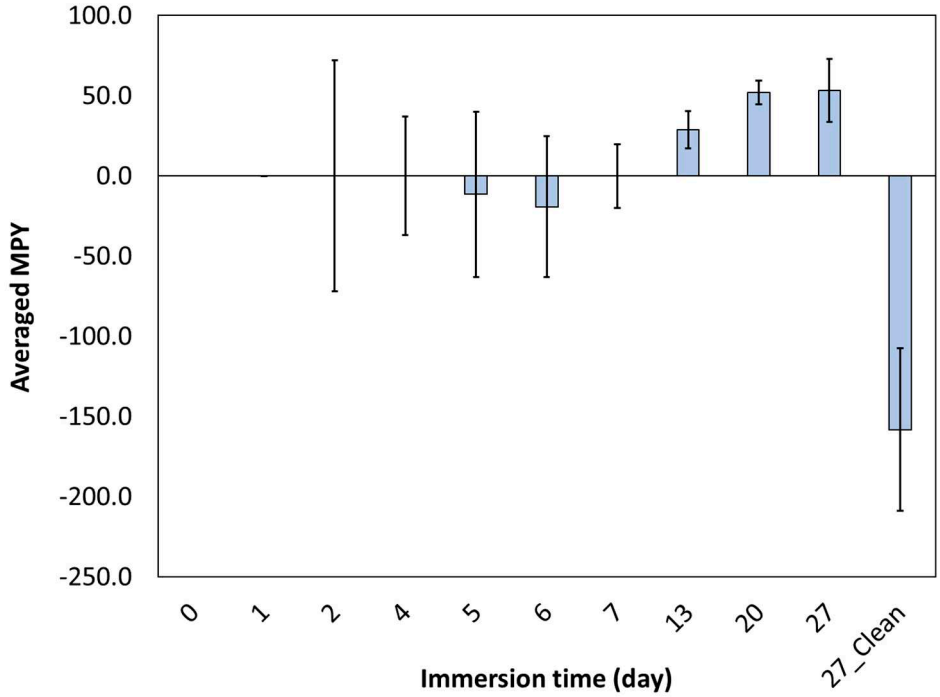

(b)

Figure 7. (a) The corrosion rate and (b) the averaged corrosion rate for coated samples.

Figure 8 shows the stress-lifetime curve for all samples and the average of samples PF-AM60-PLA and CF-AM60-PLA compared to samples PF-AM60 and CF-AM60. Basquin equation is shown in Equation 2 [54]. In this regard, $(\sigma_f^{'})$ is the coefficient of fatigue strength, (b) is the exponent of fatigue strength, and N_f is the fatigue lifetime. These coefficients are reported in Table 4.

$$\sigma_a = \sigma_f^{'}(2N_f)^b \quad (2)$$

According to Table 4, R^2 for all samples is within the acceptable range. Only in CF-AM60-PLA samples, the value of R^2 has decreased. Some of these samples were highly corroded compared to their similar samples. These samples are shown in Figure 8 (a). Because of that, their corrosion fatigue lifetime has been greatly reduced.

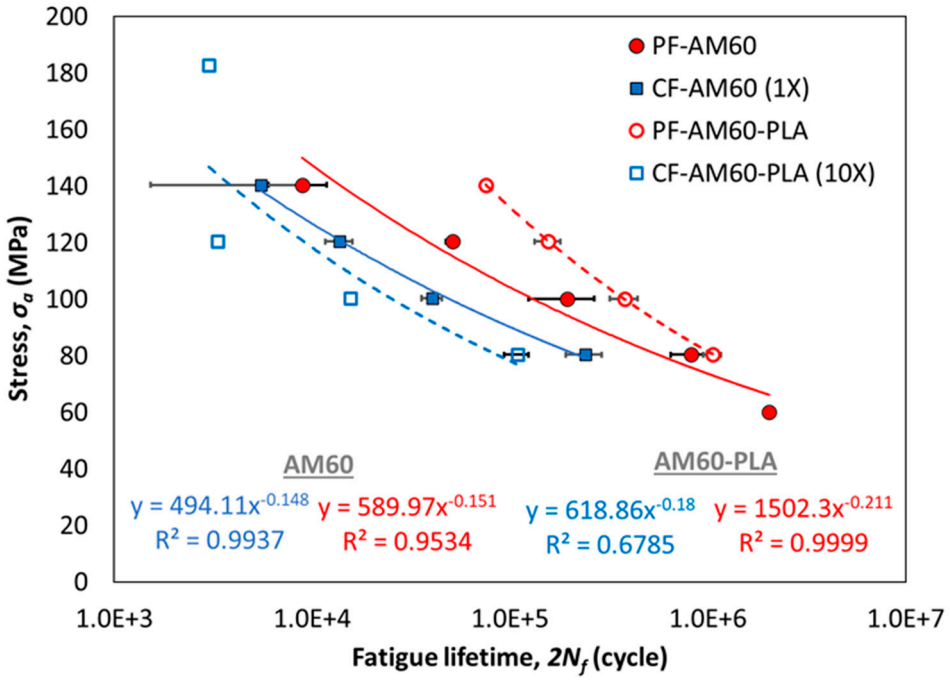

(a)

Preprints (www.preprints.org) | NOT PEER-REVIEWED | Posted: 25 December 2023 doi:10.20944/preprints202312.1814.v1

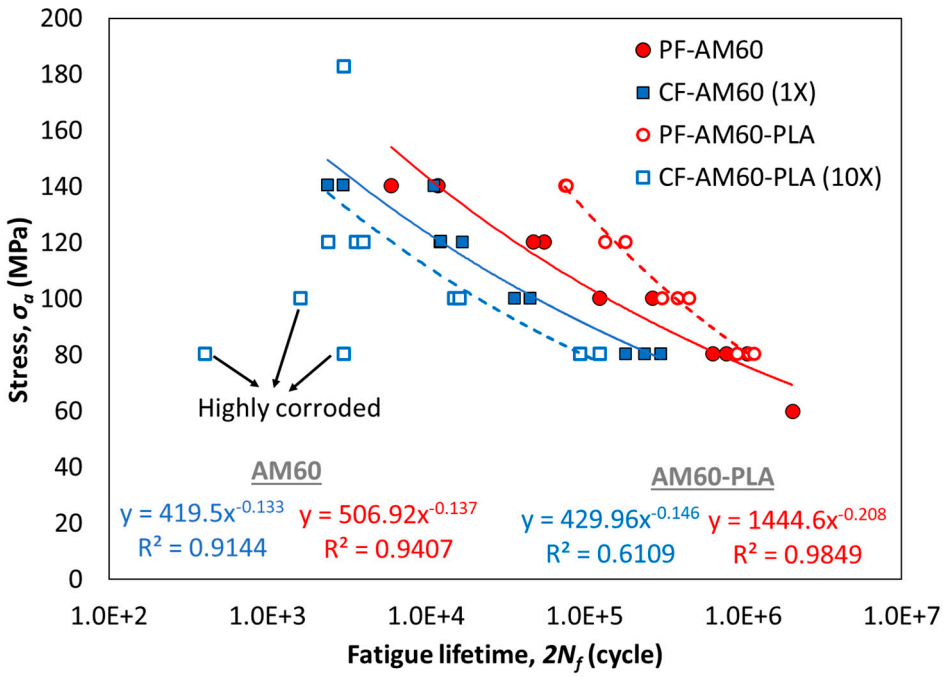

(b)

Figure 8. The stress-lifetime curves of AM60 and AM60+PLA for (a) averaged data and (b) all data.

Compared to the PF-AM60 sample, the PF-AM60-PLA sample on average had a 49% increase in fatigue lifetime. This is exactly as expected. PLA coating has increased the cross-sectional area of the sample. Therefore, fatigue resistance has increased. However, at the higher stress levels, the fatigue lifetime increased up to 67%.

The fatigue lifetime of CF-AM60-PLA specimens has decreased compared to CF-AM60 samples. However, it should be considered that 10XSBF solution was used for CF-AM60-PLA samples. In fact, despite using a 10 times stronger solution, the fatigue lifetime has decreased by only 35%.

Figure 9 shows the FESEM images of the fracture surfaces of the PF-AM60-PLA at 80 MPa of the stress level. In these figures, PLA coating and glue were seen separately. In addition, striations caused by fatigue loading were seen. Cleavage was also observed on the fracture surfaces of this specimen, which indicated the brittleness of the material [23].

In general, there are three stages containing the crack initiation, the crack growth, and the final failure due to fatigue loading. Due to bending fatigue loading, the highest stress occurs on the surface of the samples. Therefore, cracks start and grow in these areas. In the last stage, the sudden and final failure of the specimen occurs [55,56].

Figure 10 depicts the fracture surfaces of the PF-AM60-PLA at 120 MPa of the stress level. In this sample, the separation of glue and AM60 and also the separation of glue and PLA coating were observed. Similarly, striations and micro-cracks were also seen. Then, on the fracture surfaces of PLA coatings, the defects were also observed. These defects are spherical and their diameter is about 0.01 mm. One of the causes of these defects was the temperature of the nozzle during 3D printing. The temperature of 180 °C for PLA causes the material to vaporize. These vapors create bubbles in the sample. After bursting, these bubbles cause the formation of defects in the sample [57–59].

Figure 11 depicts the fracture surfaces of the CF-AM60-PLA sample at 80 MPa of the stress level. The separation of glue and sample is shown as a failure mechanism. In addition, one of the effects of corrosion is cavities and holes which were shown in research to reduce the fatigue lifetime of the specimen due to stress concentration. these products were seen in FESEM images [55,60,61]. Moreover, micro cracks were observed. These microcracks enhance the crack initiation stage in fatigue loading [56]. In research, it was shown that these cracks appear under CF conditions [62]. In another research, it was shown that the micro-cracks in the sample due to corrosion caused stress concentration and decreased the fatigue lifetime of the sample [63].

Preprints (www.preprints.org) | NOT PEER-REVIEWED | Posted: 25 December 2023 doi:10.20944/preprints202312.1814.v1

Shrinkage holes are also shown. Magnesium alloy is produced by the casting method, which is the cause of this type of shrinkage cavities. Moreover, angular cleavage plates were seen on the fracture surfaces, which indicated the brittle fracture behavior of the part.

Figure 12 illustrates the results of the EDS analysis. In this Figure, according to Table 3, the constituent elements of the SBF are shown.

Table 4. The obtained fatigue properties of AM60 magnesium alloy.

Test Conditions	All Data			Average Data		
	σ_f' (MPa)	b	R2	σ_f' (MPa)	b	R2
PF-AM60	506.92	-0.137	0.9407	589.97	-0.151	0.9534
CF-AM60	419.50	-0.133	0.9144	494.11	-0.148	0.9999
PF-AM60-PLA	1444.60	-0.208	0.9849	1502.30	-0.211	0.9999
CF-AM60-PLA	429.96	-0.146	0.6109	618.86	-0.180	0.6785

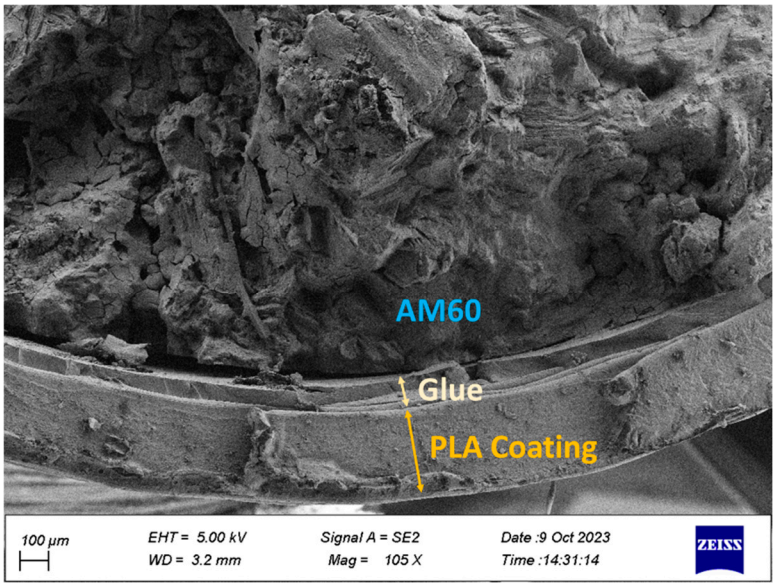

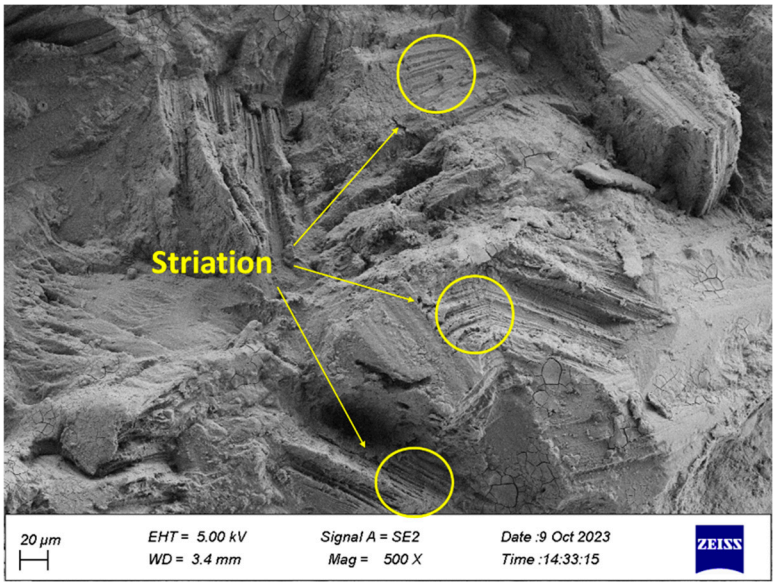

Preprints (www.preprints.org) | NOT PEER-REVIEWED | Posted: 25 December 2023 doi:10.20944/preprints202312.1814.v1

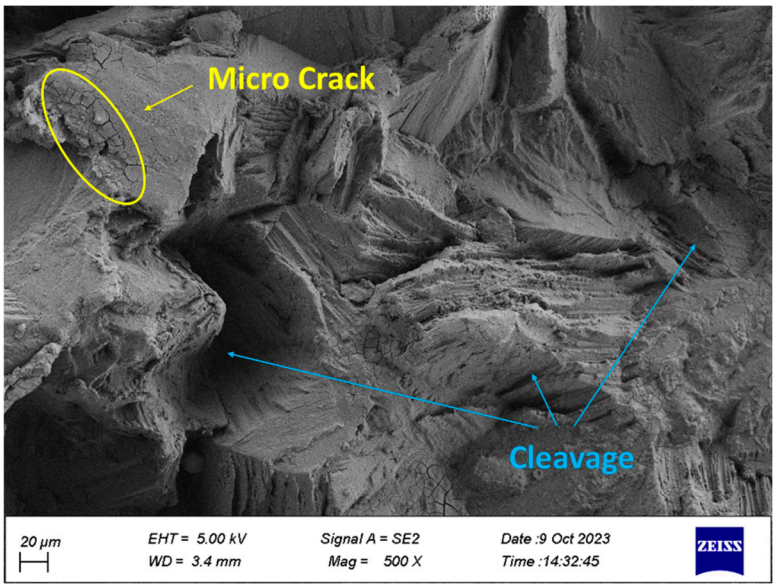

Figure 9. Fracture surface of PF-AM60-PLA at 80 MPa.

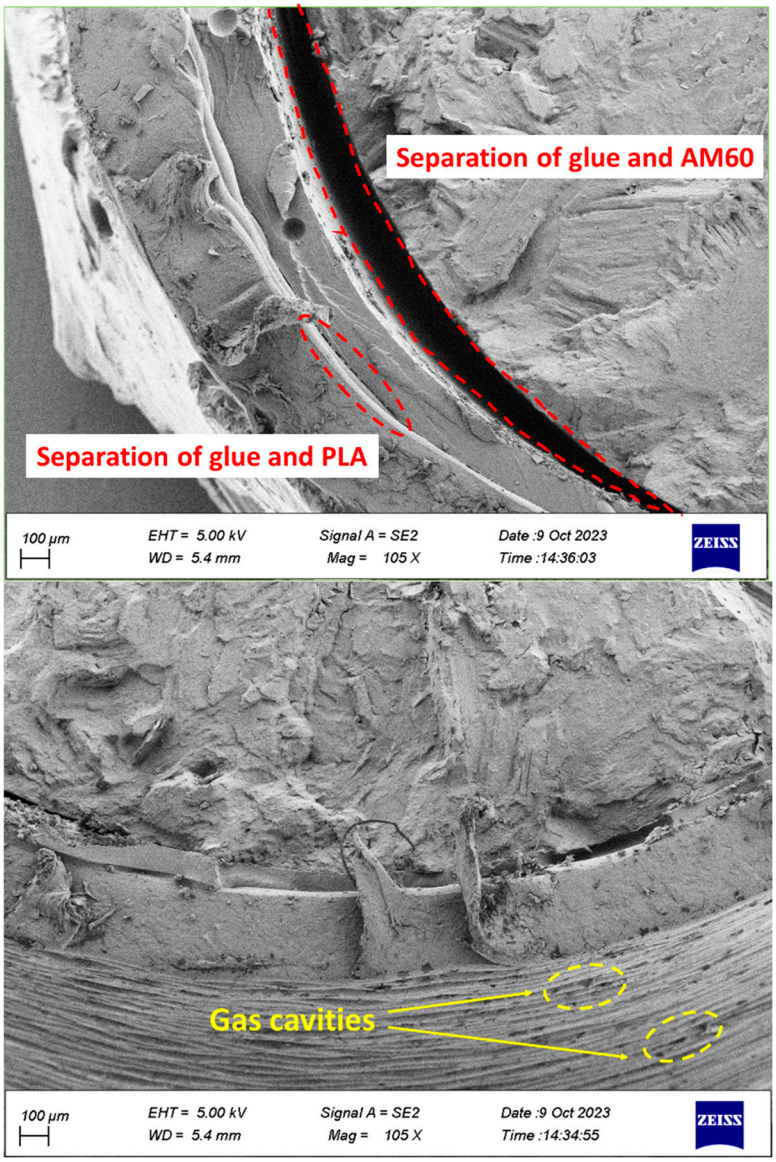

Preprints (www.preprints.org) | NOT PEER-REVIEWED | Posted: 25 December 2023 doi:10.20944/preprints202312.1814.v1

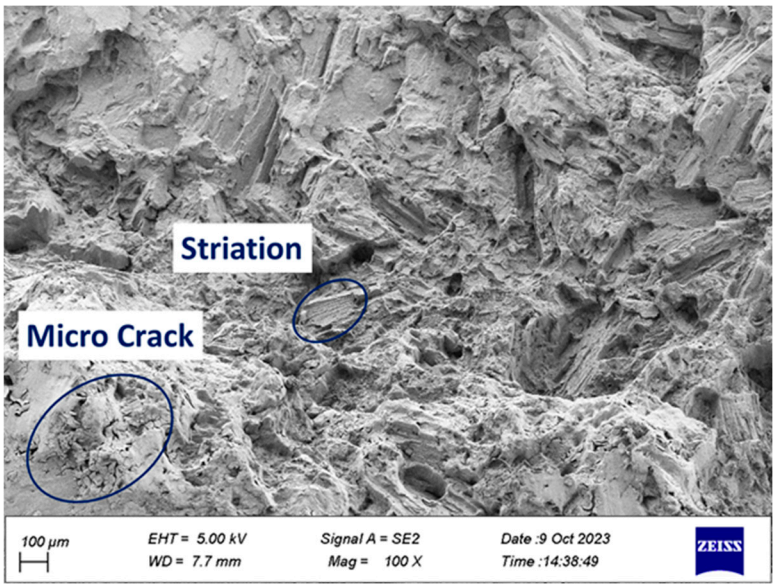

Figure 10. Fracture surface of PF-AM60-PLA at 120 MPa.

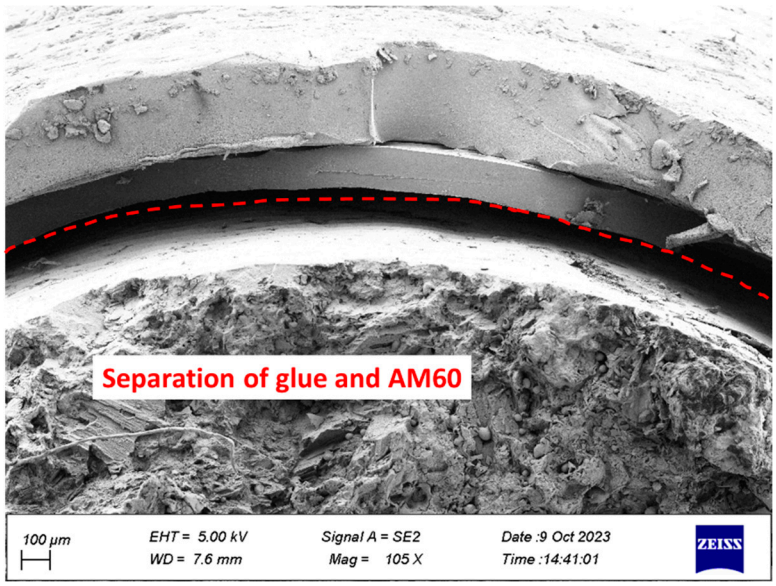

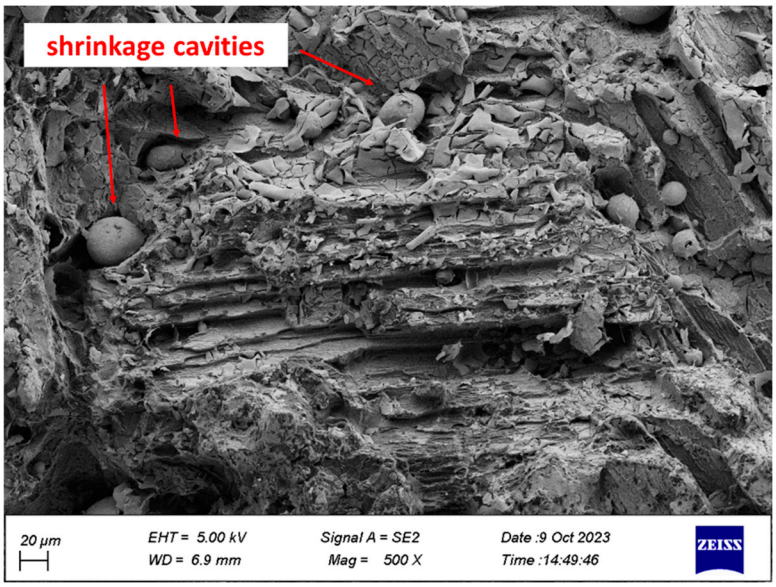

Preprints (www.preprints.org) | NOT PEER-REVIEWED | Posted: 25 December 2023 doi:10.20944/preprints202312.1814.v1

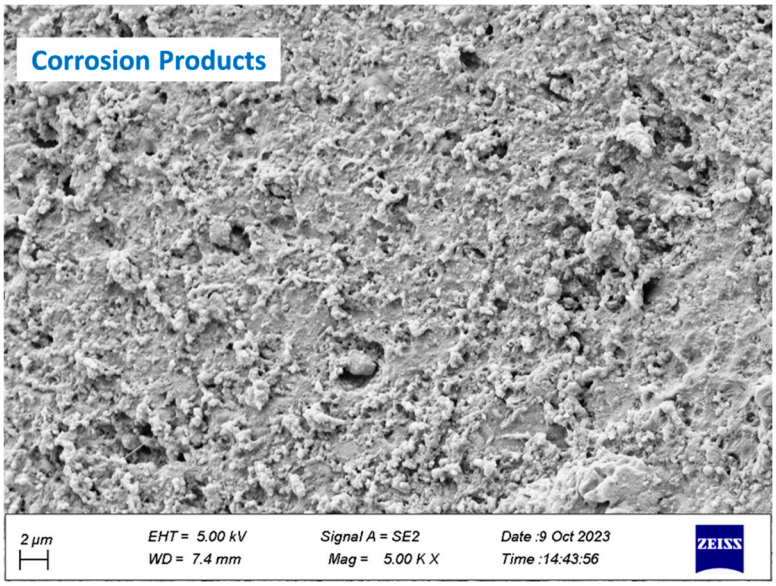

Figure 11. Fracture surface of CF-AM60-PLA at 80 MPa.

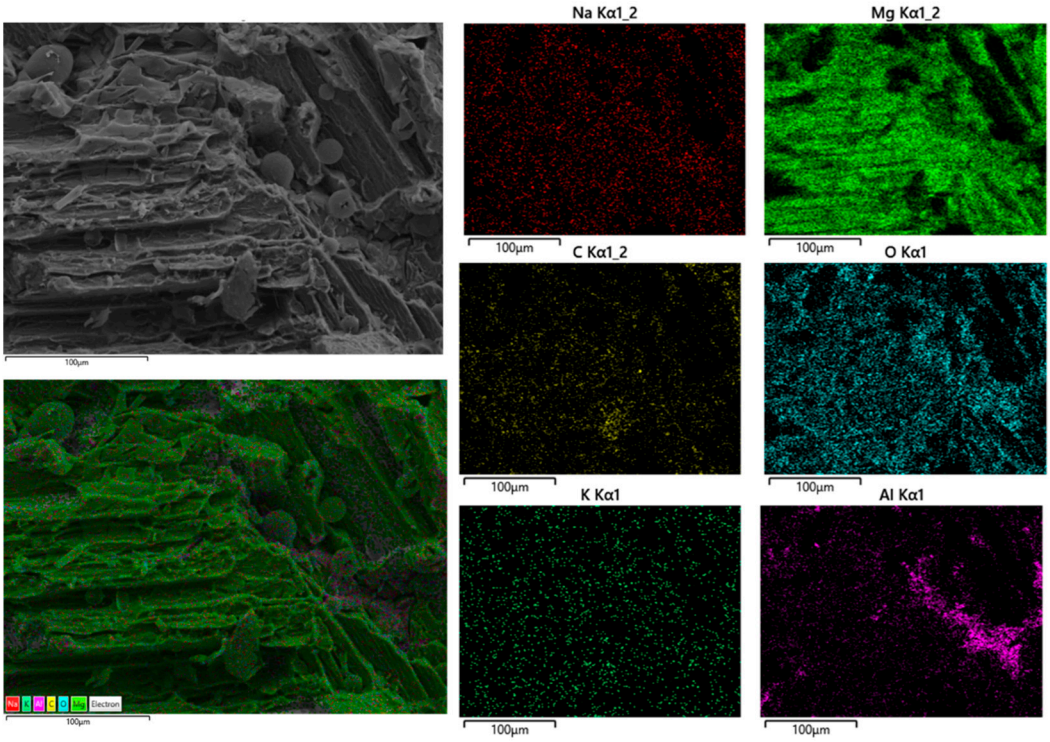

Figure 12. EDS analysis for CF-AM60-PLA at 80 MPa.

Figure 13 depicts the fracture surfaces of the CF-AM60-PLA sample at 120 MPa. In this figure, the separation of glue and sample, and also other effects such as cracks between the coating and the glue were shown. In addition, shrinkage cavities were seen, indicating improper manufacturing methods. The cleavage plates and striations were also seen. In research, it was shown that in Mg alloys at higher stress levels due to the presence of Al and Zn, the size of the holes caused by corrosion is larger, which leads to the initiation of cracks. This is while smaller holes were created at the level of less stress. These holes are connected and a crack is formed [64].

Figure 14 shows the results of the EDS analysis on the outer surface of the coating. Corrosion holes were seen on this surface. Moreover, soluble SBF elements were seen.

Preprints (www.preprints.org) | NOT PEER-REVIEWED | Posted: 25 December 2023 doi:10.20944/preprints202312.1814.v1

In general, signs of corrosion were seen only on the outer surfaces of the coating layers, and the magnesium alloy did not suffer corrosion, which is one of the advantages of using the coating.

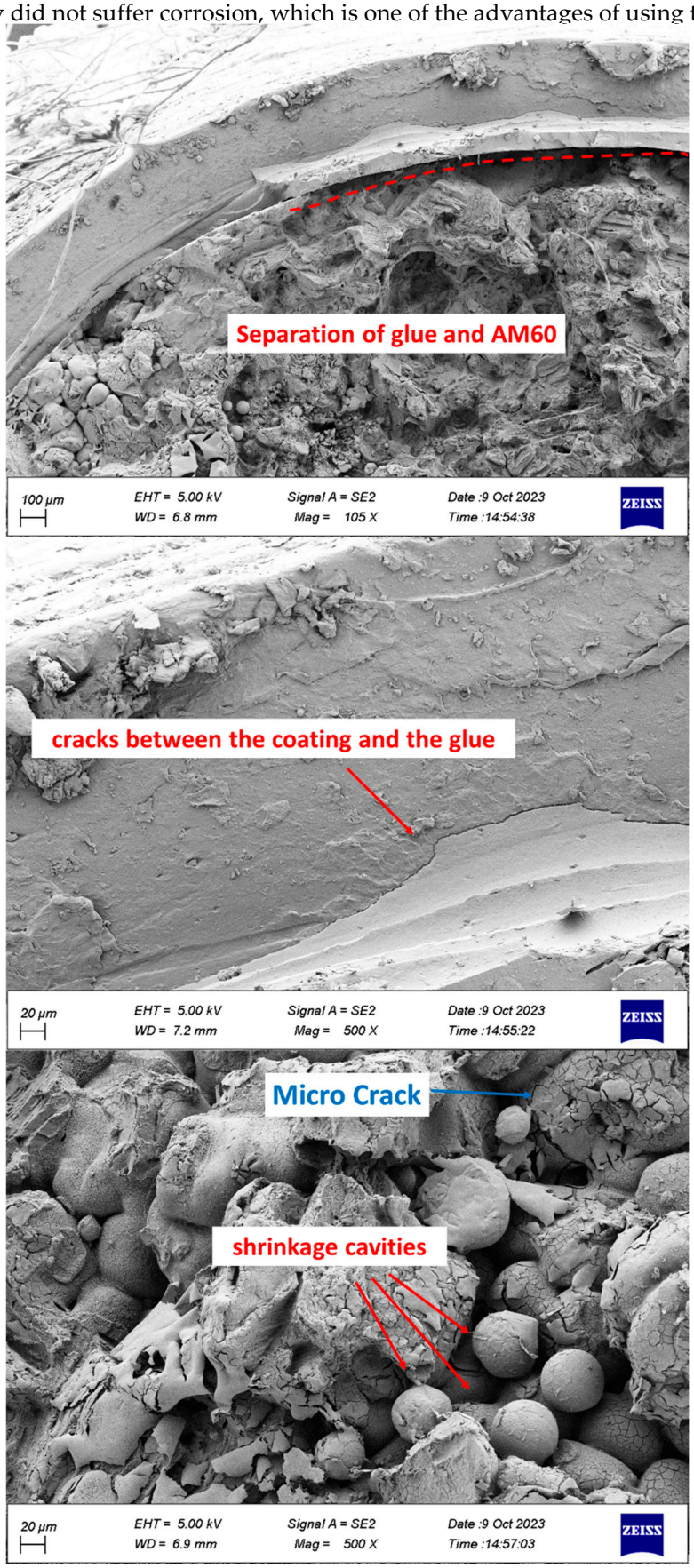

Figure 13. Fracture surface of CF-AM60-PLA at 120 MPa.

Preprints (www.preprints.org) | NOT PEER-REVIEWED | Posted: 25 December 2023 doi:10.20944/preprints202312.1814.v1

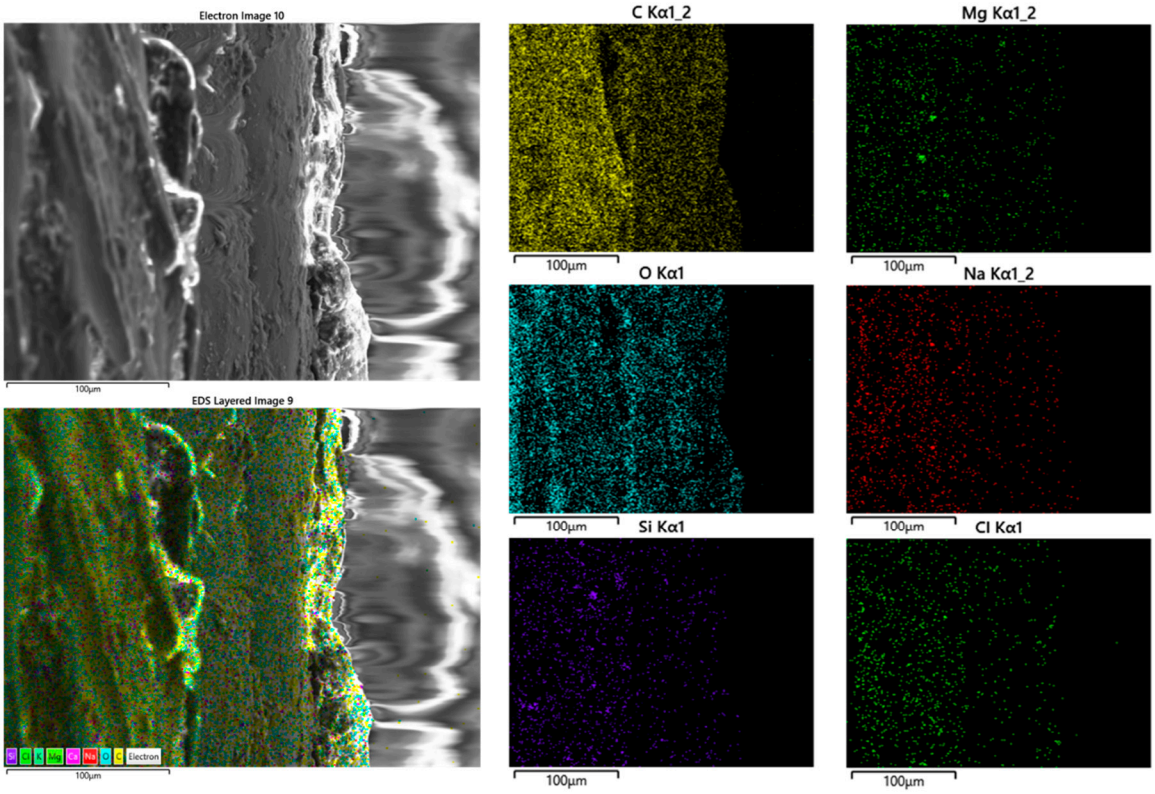

Figure 14. EDS analysis for CF-AM60-PLA at 120 MPa.

4. Conclusions

In the present research, the pure fatigue behaviors of magnesium alloy with polylactic acid (PLA) coating (PF-AM60-PLA) and the corrosion fatigue behaviors of magnesium alloy with PLA coating (CF-AM60-PLA) were investigated. The polymer coating was made of PLA and was made by additive manufacturing method (3D-printing). These covers were attached to the standard sample with a glue. Then, the specimens were immersed in the 10X SBF for 27 days. After that, the rotary bending fatigue testing device was used to evaluate the high-cycle fatigue behaviors. Finally, the fracture surfaces of the specimens were checked with FESEM images. The obtained experimental results show,

- Due to corrosion, the weight of the sample decreased by 35%.
- The corrosion rate decreased in the first 7 days and then increased.
- Compared to the PF-AM60 sample, the PF-AM60-PLA sample on average had a 49% increase in fatigue lifetime.
- Despite using a 10 times stronger solution, the fatigue lifetime of CF-AM60-PLA samples is reduced by only 35% compared to CF-AM60 samples.
- Separation of coating from glue and glue from Mg was observed.
- Cleavage plates caused by brittle fracture and striations caused by fatigue load were seen on the failure surface.
- Corrosion products including microcracks and holes were seen on the fracture surfaces of CF samples, which caused stress concentration and crack growth.
- Holes caused by the release of gases were observed in the coating.

Author Contributions: Conceptualization, M.A.; methodology, M.A. and S.A.A.T.; software, S.A.A.T.; validation, M.A.; formal analysis, S.A.A.T.; investigation, M.A. and S.A.A.T..; resources, M.A. and S.A.A.T.; data curation, S.A.A.T.; writing—original draft preparation, S.A.A.T.; writing—review and editing, M.A.; visualization, M.A. and S.A.A.T..; supervision, M.A..; project administration, M.A.; funding acquisition, M.A.

References

1. Wu C. S., Zhang Z., Cao F. H., Zhang L. J, Zhang J. Q., and C. N. Cao, "Study on the anodizing of AZ31 magnesium alloys in alkaline borate solutions", Applied Surface Science, vol. 253, pp. 3893–3898, 2007. https://doi.org/10.1016/j.apsusc.2006.08.020.
2. Moosbrugger C., Engineering Properties of Magnesium Alloys, ASM International, 2017.
3. Zartner P., Cesnjevar R., Singer H. and Weyand M., "First successful implantation of a bio-degradable metal stent into the left pulmonary artery of a preterm baby", Catheter Cardiovascular Interventions, vol. 66, pp. 590–594, 2005. https://doi.org/10.1002/ccd.20520
4. Heublein B., Rohde R., Kaese V., Niemeyer M. and Hartung W., "A. Haverich, Bio-corrosion of magnesium alloys: a new principle in cardiovascular implant technology", Heart, vol. 89, pp. 651-656, 2003. https://doi.org/10.1136/heart.89.6.651
5. Baril G., Blanc C., and Pebere N., "AC impedance spectroscopy in characterizing time-dependent corrosion of AZ91 and AM50 magnesium alloys characterization with respect to their microstructures", Journal of The Electrochemical Society, vol. 148, no. 12, 2001. https://doi.org/10.1149/1.1415722
6. Staiger M. P., Pietak A. M., Huadmai J. and Dias G., "Magnesium and its alloys as orthopedic biomaterials: A review", Biomaterials, vol. 27, no. 9, pp. 1728–1734, 2006. https://doi.org/10.1016/j.biomaterials.2005.10.003
7. Song Y., Liu D., Tang W., Dong K., Shan D. and Han E., "Comparison of the corrosion behavior of AM60 Mg alloy with and without self-healing coating in atmospheric environment", Journal of Magnesium and Alloys. vol. 9, pp. 1220–1232, 2021. https://doi.org/10.1016/j.jma.2020.05.018
8. Liu W., Cao F., Jia B., Zheng L., Zhang J., Cao C., and Li X., "Corrosion behavior of AM60 magnesium alloys containing Ce or La under thin electrolyte layers. Part 2: Corrosion product and characterization", Corrosion Science. vol. 52, pp. 639–650, 2010. https://doi.org/10.1016/j.corsci.2009.10.030
9. Matsubara H., Ichige Y., Fujita K., Nishiyama H., and Hodouchi K., "Effect of impurity Fe on corrosion behavior of AM50 and AM60 magnesium alloys", Corrosion Science, vol. 66, pp. 203–210, 2013. https://doi.org/10.1016/j.corsci.2012.09.021
10. Xie Z., Luo Z., Yang Q., Chen T., Tan S., Wang Y., and Luo Y., "Improving anti-wear and anti-corrosion properties of AM60 magnesium alloy by ion implantation and Al/AlN/CrAlN/CrN/MoS2 gradient duplex coating", Vacuum. vol. 101, pp. 171–176, 2014. https://doi.org/10.1016/j.vacuum.2013.09.002
11. Kumar D., "Effect of hydroxyapatite (HA) addition on microstructure, corrosion resistance of AZ91D", AJ62 and AM60 alloys, vol. 50, pp. 582-584, 2022.
12. Chenghao L., Shusen W., Naibao H., Zhihong Z., Shuchun Z., and Jing R., "Effects of Lanthanum and Cerium Mixed Rare Earth Metal on Abrasion and Corrosion Resistance of AM60 Magnesium Alloy Liang, Rare Metal Materials and Engineering". vol. 44, no. 3, pp. 521–526, 2015. https://doi.org/10.1016/S1875-5372(15)30031-X
13. Ikpi M.E., Dong J., and Ke W., "Electrochemical Investigation of the Galvanic Corrosion of AM60 and AD62 Magnesium Alloy in 0.1 M NaCl Solution Magdalene", International journal of electrochemical science. vol. 10, pp. 552–563, 2015.
14. Liu D., Song Y., Shan D., and Han E., "Comparison of the inhibition effect of four inhibitors on the corrosion behavior of AM60 magnesium alloy", International Journal of Electrochemical Science, vol. 13, pp. 2219–2235, 2019. https://doi.org/10.20964/2018.03.23
15. Jin-ling Z., Yang-li L., Jing Z., Zhi-yong F., and She-bin W., "Kinetic study on the corrosion behavior of AM60 magnesium alloy with different Nd contents", Journal of Alloys and Compounds. vol. 629, pp. 290–296, 2015. https://doi.org/10.1016/j.jallcom.2014.12.143
16. Akbaripanah F., Fereshteh-Saniee F., Mahmudi R., and Kim H.K., "The influences of extrusion and equal channel angular pressing (ECAP) processes on the fatigue behavior of AM60 magnesium alloy", Materials Science & Engineering A. vol. 565, pp. 308–316, 2013. https://doi.org/10.1016/j.msea.2012.12.062
17. Khan S.A., Miyashita Y., Mutoh Y., and Koike T., "Fatigue behavior of anodized AM60 magnesium alloy under humid environment", Materials Science and Engineering: A, vol. 498, pp.377-383, 2008. https://doi.org/10.1016/j.msea.2008.08.015
18. Hiromoto S., Tomozawa M., and Maruyama N., "Fatigue property of a bioabsorbable magnesium alloy with a hydroxyapatite coating formed by a chemical solution deposition", Journal of the Mechanical Behavior of Biomedical Materials. vol. 25, p. 2013. https://doi.org/10.1016/j.jmbbm.2013."04.021
19. Singh Raman R.K., Jafari S., and Harandi S.E., "Corrosion fatigue fracture of magnesium alloys in bioimplant applications: A review", Engineering Fracture Mechanics, vol. 137, pp.97-108, 2015. https://doi.org/10.1016/j.engfracmech.2014.08.009
20. Uematsu Y., Kakiuchi T., Teratani T., Harada Y., and Tokaji K., "Improvement of corrosion fatigue strength of magnesium alloy by multilayer diamond-like carbon coatings, Improvement of corrosion fatigue strength of magnesium alloy by multilayer diamond-like carbon coatings", vol. 205, pp.2778-2784, 2011. https://doi.org/10.1016/j.surfcoat.2010.10.040

21. AlamKhan S., Bhuiyan M.S., Miyashita Y., Mutoh Y., and Koike T., "Corrosion fatigue behavior of die-cast and shot-blasted AM60 magnesium alloy", Materials Science and Engineering A. vol. 528, pp. 1961–1966, 2011. https://doi.org/10.1016/j.msea.2010.11.033
22. Ishihara S., Namito T., Notoya H., and Okada A., "The corrosion fatigue resistance of an electrolytically-plated magnesium alloy", International Journal of Fatigue, vol. 32, pp. 1299-1305, 2010. https://doi.org/10.1016/j.ijfatigue.2010.01.011
23. Talesh S.A.A., and Azadi M., "High-cycle fatigue testing on AM60 magnesium alloy samples for as-received and pre-corroded conditions in simulated body fluid", Journal of Materials Research and Technology. vol. 27, pp. 1922–1934, 2023. https://doi.org/10.1016/j.jmrt.2023.10.078
24. Antunes R.A., and De Oliveira M.C.L, "Corrosion fatigue of biomedical metallic alloys: Mechanisms and mitigation", Acta Biomaterialia. vol. 8, pp. 937–962, 2012. https://doi.org/10.1016/j.actbio.2011.09.012
25. Delavar H., Mostahsan A.J., and Ibrahim H., "Corrosion and corrosion-fatigue behavior of magnesium metal matrix composites for bio-implant applications: A review", Journal of Magnesium and Alloys. vol. 11, pp. 1125–1161, 2023. https://doi.org/10.1016/j.jma.2023.04.010
26. Yadav V.K., Gaur V., and Singh I.V., "Corrosion-fatigue behavior of welded aluminum alloy 2024-T3", International Journal of Fatigue. vol. 173, pp. 107675, 2023. https://doi.org/10.1016/j.ijfatigue.2023.107675
27. Shi Y., Yang L., Zhang Q., Zhu X., Song Z., and Liu H., "A novel MAO-PLA coating on zinc alloy for potential orthopedic implant material", Materials Letters. vol. 317, 132058, 2022. https://doi.org/10.1016/j.matlet.2022.132058
28. Anand N., and Pal K., "Evaluation of biodegradable Zn–1Mg–1Mn and Zn–1Mg–1Mn-1HA composites with a polymer-ceramics coating of PLA/HA/TiO2 for orthopaedic applications", Journal of the Mechanical Behavior of Biomedical Materials. vol. 136, 105470, 2022. https://doi.org/10.1016/j.jmbbm.2022.105470
29. Wang A., Venezuela J., and Centre M.S.D., "Enhancing the corrodibility of biodegradable iron and zinc using poly (lactic) acid (PLA) coating for temporary medical implant applications", Progress in Organic Coatings journal. vol. 174, 107301, 2023. https://doi.org/10.1016/j.porgcoat.2022.107301
30. Beyzavi A.H., Azadi M., Azadi M., Dezianian S., and Talebsafa V., "Bio-polymer coatings fabricated on AM60 magnesium alloys by fused deposition modeling 3D-printing to investigate electrochemical behavior", Materials Letters. vol. 337,133935, 2023. https://doi.org/10.1016/j.matlet.2023.133935
31. ASTM Standard G-31, Standard Practice for Laboratory Immersion Corrosion Testing of Metals, Annual Book of ASTM Standards, ASTM International West Conshohocken, USA, 2021
32. Simulated body fluid catalog, Pardis Pajouhesh Fanavaran Yazd Company, Yazd Science and Technology Park, Yazd, Iran, 2023
33. Rezanezhad S., and Azadi M., "Amazing epsilon-shaped trend for fretting fatigue characteristics in AM60 magnesium alloy under stress-controlled cyclic conditions at bending loads with zero mean stress", Plos One, vol. 18, 0281263, 2023. https://doi.org/10.1371/journal.pone.0281263
34. Dezianian S., and Azadi M., "Multi-Material Metamaterial Topology Optimization to Minimize the Compliance and the Constraint of Weight: Application of Non-Pneumatic Tire Additive-Manufactured with PLA/TPU Polymers", Polymers, vol. 15, 1927, 2023. https://doi.org/10.3390/polym15081927
35. Dezianian S., Azadi M., and Razavi S.M.J., "Topology optimization on metamaterial cells for replacement possibility in non-pneumatic tire and the capability of 3D-printing", Plos One, vol. 18, 2023. https://doi.org/10.1371/journal.pone.0290345
36. Rezanezhad S., and Azadi M., "Impact of 3D-printed PLA coatings on the mechanical and adhesion properties of AM60 magnesium alloys", Composites Part C, vol. 12, 100415, 2023. https://doi.org/10.1016/j.jcomc.2023.100415
37. Azadi M., Dadashi A., Dezianian S., Kianifar M., Torkaman S., and Chiyani M., "High-cycle bending fatigue properties of additive-manufactured ABS and PLA polymers fabricated by fused deposition modeling 3D-printing." Forces Mech, vol.3, 100016, 2021. https://doi.org/10.1016/j.finmec.2021.100016
38. Rudawska A., Sarna-Boś K., Rudawska A., Różyło-Kalinowska I., and Chałas R., "Biological and chemical properties of cured epoxy resins", Research Square, 2021. https://doi.org/10.21203/rs.3.rs-992480/v1
39. Muñoz M., Torres B., Mohedano M., Matykina E., Arrabal R., López A.J., and Rams J., "PLA deposition on surface treated magnesium alloy: Adhesion, toughness and corrosion behavior" Surf Coatings Technol, vol. 388, 125593, 2020. https://doi.org/10.1016/j.surfcoat.2020.125593
40. Azadi M., and Parast M., "Data analysis of high-cycle fatigue testing on piston aluminum-silicon alloys under various conditions: Wear, lubrication, corrosion, nano-particles, heat-treating, and stress", Data in Brief, vol. 41, 107984, 2022. https://doi.org/10.1016/j.dib.2022.107984
41. Metallic materials - rotating bar bending fatigue testing, Standard No. ISO 1143, ISO International Standard, 2010
42. Rotating bar bending fatigue test, Standard No. DIN EN 50113, DIN Standard, 1982
43. Standard practice for laboratory immersion corrosion testing of metals, ASTM International, Designation: G 31 – 72 (Reapproved 2004).

44. Oliya A. Y. P., Azadi M., Parast M. S. A., and Mokhtarishirazabad M., "Effect of Heat-Treating on Microstructure and High Cycle Bending Fatigue Behavior of AZ91 and AZE911 Magnesium Alloys", Advances in Materials Science and Engineering, pp. 1–11, 2022. https://doi.org/10.1155/2022/4030062
45. Hodaeian H., Degradation of Pure Magnesium Alloys, 2013.
46. Guo Z., Yang C., Zhou Z., Chen S., and Li F., "Characterization of biodegradable poly (lactic acid) porous scaffolds prepared using selective enzymatic degradation for tissue engineering", Royal society of chemistry Advances, vol. 7, 34063, 2017. https://doi.org/10.1039/C7RA03574H
47. Hasanpur E., Ghazavizadeh A., Sadeghi A., and Haboussi M., "In vitro corrosion study of PLA/Mg composites for cardiovascular stent applications", Journal of the Mechanical Behavior of Biomedical Materials, vol. 124, 104768, 2021. https://doi.org/10.1016/j.jmbbm.2021.104768
48. Balogova A., Trebunova M., Izarikova G., Kascak L., Mitrík L., Klimova J., Feranc J., Modrak M., Hudak R., and Zivcak J., "In Vitro Degradation of Specimens Produced from PLA/PHB by Additive Manufacturing in Simulated Conditions", Polymers, vol.13, 1542, 2021. https://doi.org/10.3390/polym13101542
49. Redondo F., Giaroli M., Ciolino A., and Ninago M., "Preparation of Porous Poly (Lactic Acid)/Tricalcium Phosphate Composite Scaffolds for Tissue Engineering", Biointerface Research in Applied Chemistry, vol. 12, 2022, pp. 5610 – 5624, 2021.
50. Alksne M., Kalvaityte M., Simoliunas E., Rinkunaite I., Gendviliene I., Locs J., Rutkunas V., and Bukelskiene V., "In vitro comparison of 3D printed polylactic acid/hydroxyapatite and polylactic acid/bio-glass composite scaffolds: Insights into materials for bone regeneration", Journal of the Mechanical Behavior of Biomedical Materials, vol. 104, 103641, 2020. https://doi.org/10.1016/j.jmbbm.2020.103641
51. Chor A., Gonçalves R., Costa A., Farina M., Ponche A., Sirelli L., Schrodj G., Gree S., Andrade L., Anselme K., and Dias M., "In Vitro Degradation of Electro-spun Poly (Lactic-Co-Glycolic Acid) (PLGA) for Oral Mucosa Regeneration", Polymers, vol. 12, 1853, 2020. https://doi.org/10.3390/polym12081853
52. Voicu M.E., Demetrescu I., Dorobantu A., Enachescu M., Buica G.O., and Ionita D., "Interaction of Mg Alloy with PLA Electro-spun Nanofibers Coating in Understanding Changes of Corrosion", Nanomaterials, vol. 12, 12081369, 2022. https://doi.org/10.3390/nano12081369
53. Shi P., Niu B., Shanshan E., Chen Y., and Li Q., "Preparation and characterization of PLA coating and PLA/MAO composite coatings on AZ31 magnesium alloy for improvement of corrosion resistance", Surface and Coatings Technology, vol. 262, pp. 26-32, 2015. https://doi.org/10.1016/j.surfcoat.2014.11.069
54. Basquin O.H., "The exponential law of endurance tests", Proceeding of American Society of Testing and Materials, 1910.
55. Ghazizadeh E., Jabbari A.H., and Sedighi M., "In vitro corrosion fatigue behavior of biodegradable Mg/HA composite in simulated body fluid.", Journal of Magnesium and Alloys, vol. 9, pp.2169-2184, 2021. https://doi.org/10.1016/j.jma.2021.03.027
56. Stephens R., Fatemi A., Stephens R., and Fuchs H., "Metal fatigue in engineering", John Wiley and Sons, 2000.
57. Mokhtarishirazabad M., Azadi M., Farrahi G.H., Winter G., and Eichlseder W., "Improvement of high temperature fatigue lifetime in AZ91 magnesium alloy by heat treatment", Materials Science & Engineering A, vol. 588, pp. 357-365, 2013. https://doi.org/10.1016/j.jma.2021.03.027
58. Farrahi G.H., Azadi M., Winter G., and Eichlseder W., "A new energy-based isothermal and thermo-mechanical fatigue lifetime prediction model for aluminum–silicon–magnesium alloy", Fatigue & Fracture of Engineering Materials & Structures, vol. 36, pp. 1323-1335, 2013. https://doi.org/10.1111/ffe.12078
59. Jiang L., Xu F., Xu Z., Chen Y., Zhou X., Wei G., and Ge H., "Biodegradation of AZ31 and WE43 Magnesium Alloys in Simulated Body Fluid", International journal of electrochemical science, vol. 10, pp. 10422-10432, 2015. https://doi.org/10.1016/S1452-3981(23)11268-5
60. Liu M., Wang J., Zhu S., Zhang Y., Sun Y., Wang L., and Guan S., "Corrosion fatigue of the extruded Mg-Zn-Y-Nd alloy in simulated body fluid", Journal of Magnesium and Alloys, vol. 8, pp. 231-240, 2020. https://doi.org/10.1016/j.jma.2019.09.009
61. Azadi M., Aroo H., and Parast M.S.A., "Comparing of high-cycle fatigue lifetimes in un-corroded and corroded piston aluminum alloys in diesel engine applications", Archives of Foundry Engineering, vol.21, pp. 89-94, 2021. https://doi.org/10.24425/afe.2021.136083
62. Parast M.S.A., and Azadi M., "A short evaluation of simultaneous corrosion fretting fatigue behaviors in piston aluminum-silicon alloys considering effects of nano-particles and heat-treating", International Journal of Fatigue, vol. 168, 107403, 2023. https://doi.org/10.1016/j.ijfatigue.2022.107403

63. Nan N.Y., Ishihara S., and Goshima T., "Corrosion fatigue behavior of extruded magnesium alloy AZ31 in sodium chloride solution", International Journal of Fatigue, vol.30, pp.1181-1188, 2008. https://doi.org/10.1016/j.ijfatigue.2007.09.005
64. Bhuiyan M.S., Mutoh Y., Murai T., and Iwakami S., "Corrosion fatigue behavior of extruded magnesium alloy AZ80-T5 in a 5% NaCl environment", Engineering Fracture Mechanics, vol. 77, pp. 1567-1576, 2010. https://doi.org/10.1016/j.engfracmech.2010.03.032